On the origin and application of the Bruggeman correlation for analysing transport phenomena in electrochemical systems

Bernhard Tjaden[1,4], Samuel J Cooper[2,4], Daniel JL Brett[1], Denis Kramer[3] and Paul R Shearing[1]

CrossMark

The widely used Bruggeman equations correlate tortuosity factors of porous media with their porosity. Finding diverse application from optics to bubble formation, it received considerable attention in fuel cell and battery research, recently. The ability to estimate tortuous mass transport resistance based on porosity alone is attractive, because direct access to the tortuosity factors is notoriously difficult. The correlation, however, has limitations, which are not widely appreciated owing to the limited accessibility of the original manuscript. We retrace Bruggeman's derivation, together with its initial assumptions, and comment on validity and limitations apparent from the original work to offer some guidance on its use.

Addresses
[1] Electrochemical Innovation Lab, Department of Chemical Engineering, UCL, London WC1E 7JE, UK
[2] Department of Material, Imperial College London, South Kensington, London SW7 2AZ, UK
[3] Faculty of Engineering and the Environment, University of Southampton, University Road, Southampton SO17 1BJ, UK

Corresponding author: Kramer, Denis (D.Kramer@soton.ac.uk)
[4] These authors contributed equally to this work..

Introduction

Geometric complexity is a long-standing challenge in efficiently describing transport problems within a continuum setting. Although transport in some simple geometries is analytically solvable, in even 'mildly' more complex geometries transport must be treated numerically. Porous media can be found in applications as diverse as heterogeneous catalysis, energy technologies including fuel cells and batteries, geology and the oil industry. It is surprisingly easy to envision a porous geometry that would confound today's formidable super-computers, due to their heterogeneous networks with relevant length scales spanning several orders of magnitude.

A number of important transport problems have the ansatz

$$\dot{\mathbf{F}} \propto \nabla \mathbf{C}, \tag{1}$$

which connects a flux, $\dot{\mathbf{F}}$, linearly to a driving force, taken to be the gradient of a potential, $\nabla \mathbf{C}$. Fourier's law (heat transport), Ohm's law (charge transport), Fick's law (diffusive transport) and Darcy's law (hydraulic transport), among others, all express a flux as a linear response to a potential gradient. The same linear relation is encountered in problems related to electromagnetism (permeability) and fluid dynamics (viscosity). Laplace's equation follows from flux conservation if the proportionality factor is a constant (i.e. it does not vary in space or time):

$$\nabla \dot{\mathbf{F}} = \nabla^2 \mathbf{C} = 0. \tag{2}$$

Solution of the transport problem is in some cases straightforward as analytical solutions exist for a number of simple geometries and boundary conditions [1]. More complex geometries and/or boundary conditions call for numerical methods such as finite difference or finite element approaches. Owing to their simplicity, effective medium theories, which aim to absorb local complexity into effective transport coefficients, are popular. One such relationship was developed by D.A.G. Bruggeman who proposed a method to average locally for a number of geometries [2], building on earlier work by Lorentz [3], Lorenz [4] and Rayleigh [5]. The Bruggeman correlation is widely used in different fields such as optics [6], electromagnetics [7], in calculating thermal [8] and electrical properties [9] as well as in electrochemical research [10,11,12•] and in effective medium approximation models [13].

Notably, the simplicity with which it is possible to extract effective transport parameters for a porous medium, based solely on knowledge of its porosity, has made this an attractive method. However, Bruggeman's original work, which dates back to 1935 and is published in German, is not readily available in the English-speaking scientific literature today. Moreover, Bruggeman did not explicitly address the special case, which leads to the

simple analytic expression relating the porosity to the tortuosity factor which has become popular to describe transport in porous media (cf., Eqn 17). In consequence, there is some disagreement and general confusion in the literature about the validity and applicability of Bruggeman's equation.

In an attempt to clarify the application and limitations of this method, we retrace Bruggeman's reasoning, leading to the general formulation of his model for simultaneous transport in a number of intimately mixed bodies (cf. Eqn 4) and highlight the connection to a popular form of his equation for transport in one medium (cf. Eqn 17).

Motivation

The obstruction to free-space transport caused by the geometry of a sample is commonly expressed by the tortuosity factor. Several detailed reviews [14–16] have surveyed the literature in this area. Besides the Bruggeman correlation, many other theoretical and empirical equations have been developed to approximate the tortuosity factor. Among these, Maxwell's porosity–tortuosity factor relation [17] is probably the oldest and is still widely used for analysis purposes [18,19].

There is substantial contemporary interest in the application of the concept of tortuosity factor as a coarse-grained expression of geometric complexity to model mass transport in porous media. For example, the provision of reactant gases to electro-catalytically active sites is known to limit the performance of fuel cells under high current densities [20]. The extent of voltage loss due to mass transport limitations is directly related to the microstructure of porous fuel cell gas diffusion electrodes and transport layers. The tortuosity factor, consequently, plays a vital role in modelling fuel cell behaviour [21–23]. Similarly, the rate of transport of Li^+ through the electrolyte in a flooded porous media is directly associated with the microstructure in Li-ion battery electrodes [10,12•]. In addition, tortuosity factor is an input parameter in 'Newman-type' models of battery performance [24]. Hence, understanding the effect of porous microstructures in electrochemical systems is vital to improve cell manufacturing methods of support and electrode layers and increase system efficiency across the whole operating range.

The direct measurement of the tortuosity factor is non-trivial, and consequently simplified effective medium correlations have been widely applied. In recent years, the development and proliferation of advanced three-dimensional imaging techniques has provided for the first time a quantified microstructural map of complex pore geometries [25]. Subsequent combination of tomography data with image-based models provides an alternative route to tortuosity factor determination and a compelling opportunity to directly evaluate the accuracy of effective

medium correlations. Recent studies report conflicting results on the validity of the Bruggeman equation: whilst in some instances, tomography-based microstructural simulations agree with the Bruggeman correlation [26,10], substantial disagreement was observed in other cases [27,28•]. It has become apparent that the characteristic shape of the analysed microstructure has considerable bearing on the validity of the Bruggeman relation. Especially, anisotropy and geometry are aspects of porous materials that are not reflected by the Bruggeman equation.

The authors believe that the existing controversy around the validity and applicability of the Bruggeman correlation is partially due to the original work being difficult to access and interpret. We, therefore, consider it worthwhile to revisit the derivation of the Bruggeman correlation and comment on selected applications to support the discussion with a better understanding of how the limitations of effective medium correlations evolve from the fundamental assumptions made to construct them.

## Tortuosity and the tortuosity factor

Before moving to the details of the Bruggeman formulation, it is important to clarify that the tortuosity, distinct from the tortuosity factor, is another parameter related to the geometry of a system. The tortuosity is the ratio of an effective path length, L_p, to the edge length of the control volume, L_{cv}, and is often introduced in the literature using a simplified 2D case, similar to one of the examples shown in Figure 1.

Epstein [29] derives a relation between these two terms in a short communication on the topic, which can be summarised as follows: the diffusion through a simple, capillary pore is proportional to its effective cross-sectional area, A_p, and inversely proportional to its length, L_p. Also, for any pore of fixed volume, doubling its length must result in a corresponding halving of the cross-sectional area. These two facts in combination suggest that the effect of a length change on transport must be squared to account for both the extra path length and the implied reduction in area. This derivation can also be reframed in terms of the area reduction or as a combination of length and area. Eqn 3 shows the relation between these various descriptions of transport obstruction and a tortuosity factor specific to capillary systems, $\tau_{capillary}$,

$$\tau_{capillary} = \left(\frac{L_p}{L_{cv}}\right)^2 = \left(\frac{\varepsilon A_{cv}}{A_p}\right)^2 = \left(\frac{\varepsilon L_p A_{cv}}{L_{cv} A_p}\right), \qquad (3)$$

where L_{cv} and A_{cv} are the length and cross sectional area of the control volume, respectively, and ε is the volume fraction of the conductive phase. As Epstein makes clear [29], this derivation is only valid when the structures considered can reasonably be described using a capillary

Figure 1
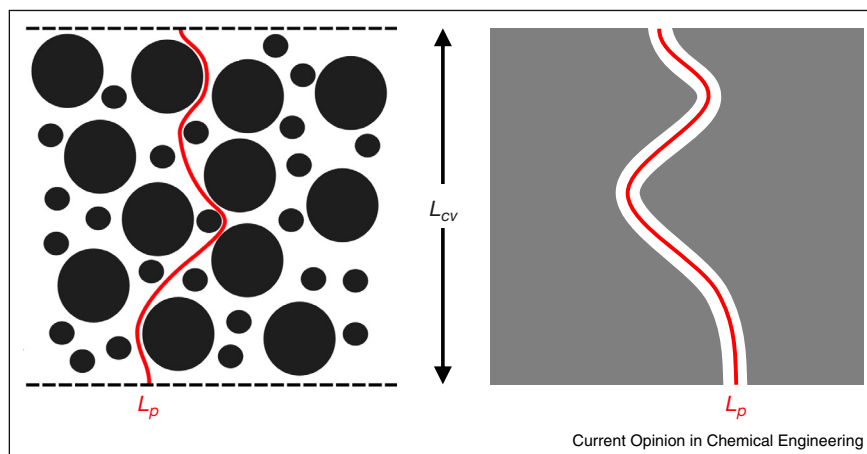
Two common illustrations of the concept of geometrical tortuosity.

model (i.e. where the cross-sectional area normal to the flow path is constant), which is rarely the case in the highly complex electrode microstructures encountered in fuel cells and batteries. Otherwise, the meaning of L_p and A_p cannot be clearly defined; as in, for example, an hour glass geometry.

The Bruggeman model
Regularly spaced and dilute inclusions
Lord Rayleigh [5] derived two formulae for effective transport coefficients of cylinders and spheres embedded into another phase on a regular quadratic (cubic) lattice. These are based on the models of Lorenz [4] and Lorentz [3] which relate the refractive index of a medium with its density. While Lorenz and Lorentz considered the consequence of molecular obstacles in the dilute limit, Lord Rayleigh investigated the more definite case of regularly spaced obstacles that cannot be regarded as small compared with the distance between them. Using D and ε to denote the transport coefficients and volume fractions of the two phases, respectively, he showed that, when $\varepsilon_1 \ll \varepsilon_2$, the effective transport coefficient is given by

$$\frac{D_{\text{eff}} - D_2}{D_{\text{eff}} + nD_2} = \lambda \frac{D_1 - D_2}{D_1 + nD_2}, \tag{4}$$

where $\lambda = \varepsilon_1/\varepsilon_2$, with $n = 2$ for spheres and $n = 1$ for cylinders.

Lord Rayleigh's paper provides insights into the use of conservation laws to treat transport problems. He used a spectral method to solve for the potentials, C_1 and C_2, inside and outside the spheres, respectively, imposing continuity of the potential and conservation of flux

$$C_1 = C_2 \quad \text{and} \quad D_1 \nabla C_1 = D_2 \nabla C_2$$

at the interface to solve for the coefficients of the series expansion.

This formulation is also consistent with boundary constriction expressions for the effective transport coefficient developed by Wiener [30]. It is, however, important to note that Eqn 4 is only strictly valid for a square array with the flux parallel to one of the lattice constants. Bruggeman expanded on this by considering random structures.

Randomly placed inclusions
Bruggeman considered a process of embedding two different phases in a sample and based his reasoning on these assumptions:

1. The sample consists of two homogeneous and isotropic phases.
2. Each phase consists of particles that are small in comparison to the sample size.
3. Each phase is randomly distributed in the sample.

Using the above assumptions connected to Rayleigh's derivation, he developed a theory based on a recursive procedure, where each step of the recursion starts with an auxiliary homogeneous medium having the target property D_{eff}. After embedding a small volume fraction, ε_1', of phase one, the aggregate is approximated as a new homogeneous medium with the transport coefficient, D_{eff}', given by Eqn 4:

$$\frac{D_{\text{eff}}' - D_{\text{eff}}}{D_{\text{eff}}' + nD_{\text{eff}}} = \varepsilon_1' \frac{D_1 - D_{\text{eff}}}{D_1 + nD_{\text{eff}}}. \tag{5}$$

Note that $\lambda \simeq \varepsilon_1$ for $\varepsilon_1 \ll \varepsilon_2$. The target property, D_{eff}, is

restored by embedding an appropriate amount ε'_2 of phase two, which leads to

$$\frac{D_{\text{eff}} - D'_{\text{eff}}}{D_{\text{eff}} + nD'_{\text{eff}}} = \varepsilon'_2 \frac{D_2 - D'_{\text{eff}}}{D_2 + nD'_{\text{eff}}}. \tag{6}$$

Adding Eqns 5 and 6 and setting $D_{\text{eff}} \simeq D'_{\text{eff}}$ leads to

$$\varepsilon'_1 \frac{D_1 - D_{\text{eff}}}{D_1 + nD_{\text{eff}}} + \varepsilon'_2 \frac{D_2 - D_{\text{eff}}}{D_2 + nD_{\text{eff}}} = 0 \tag{7}$$

This embedding procedure is repeated until the entire volume is filled with small inclusions of phases one and two, completely replacing the auxiliary homogeneous medium, as illustrated in Figure 2. Each embedding step produces an equation of the same type as Eqn 7, and summation over all steps $\varepsilon'_i + \varepsilon''_i + \cdots = \varepsilon_i$ gives

$$\varepsilon_1 \frac{D_1 - D_{\text{eff}}}{D_1 + nD_{\text{eff}}} + \varepsilon_2 \frac{D_2 - D_{\text{eff}}}{D_2 + nD_{\text{eff}}} = 0, \tag{8}$$

which is the main result of Bruggeman's considerations.

Insulating second phase

Eqn 8 is commonly used if the transport properties of both phases are comparable. A simpler relation, however, can be obtained following a slightly modified procedure if transport within one phase is negligible. This is often the case when considering mass transport through porous media. Instead of alternating between embedding small inclusions of phase one and phase two in an auxiliary homogeneous medium, a small volume, λ, will be taken out of a homogeneous effective medium, initially consisting of the homogeneous phase two (i.e., $D_{\text{eff}}^{[0]} = D_2$), and replaced with an inclusion of phase one. This process is represented in Figure 3, which shows a sequence of embedding and averaging steps. The upper row shows the true geometry, highlighting the full geometric complexity. The lower row

visualises the spheres included in each iteration first as superimposed onto the effective medium and then approximately 'dissolved' into the effective medium, with the changing effective transport property depicted by a change of opacity. The addition of particles increases the opacity (darker blue shade) of the sample volume, which reflects a reduction in the effective transport coefficient.

With $D_1 = 0$, Eqn 4 can be written as

$$\frac{D_{\text{eff}}^{[i]} - D_{\text{eff}}^{[i-1]}}{D_{\text{eff}}^{[i]} + nD_{\text{eff}}^{[i-1]}} = -\frac{\lambda}{n} \tag{9}$$

for the ith embedding step. This recurrence relation is a geometric series, leading to

$$\frac{D_{\text{eff}}^{[i]}}{D_2} = \left(\frac{n - n\lambda}{n + \lambda}\right)^i \quad \text{with} \quad D_{\text{eff}}^{[0]} = D_2. \tag{10}$$

This procedure is repeated N times until a volume fraction, ε_1, is filled with the insulating phase. A total volume $V = N\lambda$ will be replaced in the process. Taking the limit

$$\lim_{N \to \infty} \left(\frac{n - n(V/N)}{n + (V/N)}\right)^N = \exp\left(-\frac{V(1+n)}{n}\right) = \frac{D_{\text{eff}}}{D_2} \tag{11}$$

shows that D_{eff} decays exponentially with the exchanged volume. After each iteration, the effective medium will contain an increased amount of phase one. Hence, taking out a volume, λ, and replacing it with phase one will increase the volume fraction of phase one by only

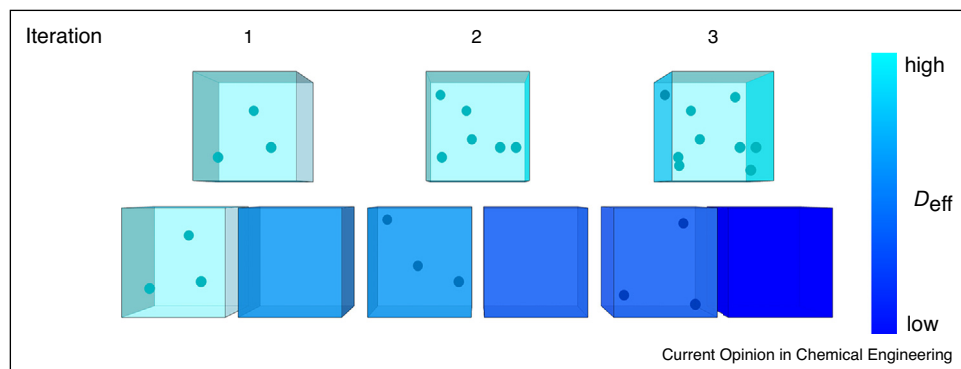$$\varepsilon_1^{[i]} - \varepsilon_1^{[i-1]} = \lambda(1 - \varepsilon_1^{[i-1]}), \tag{12}$$

because the removed volume, λ, contained a fraction $\lambda\varepsilon_1^{[i-1]}$ of phase one already. This is another geometric series leading to

Figure 2
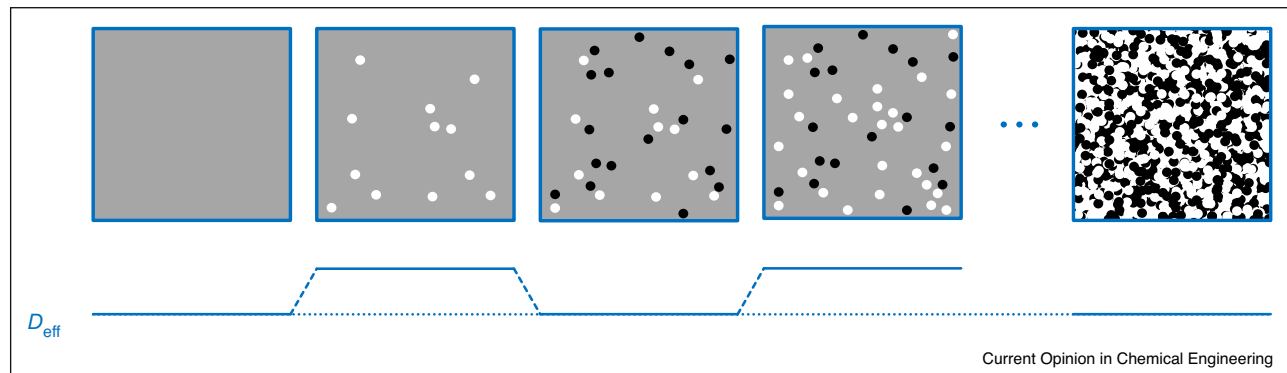
Two dimensional representation of the Bruggeman iterative method with an axis showing the change in the diffusion coefficient within each iteration compared to the target value, D_{eff}.

Figure 3

Qualitative 3D representation of adding isolating spheres into a medium resulting in an decrease of the effective transport property D_{eff}. While the upper row of volumes shows the true geometry which is changed by adding isolating spheres for each step, the lower row illustrates that after each iteration, the insulating spheres are dissolved and the effective transport property of the medium is averaged highlighted in a change in opacity.

$$\varepsilon_1^{[i]} = 1 - (1-\lambda)^i. \tag{13}$$

Taking again the limit

$$\lim_{N \to \infty} \left(1 - \left(\frac{V}{N}\right)\right)^N = \exp(-V) = 1 - \varepsilon_1 = \varepsilon_2, \tag{14}$$

introducing the result into Eqn 11 and dropping the phase index leads to the particularly simple expression

$$\frac{D_{eff}}{D} = \varepsilon^{(1+n)/n} \tag{15}$$

relating D_{eff} to the volume fraction, ε, of the transporting phase.

It is common practice to define the tortuosity factor, τ, for porous media such that

$$\frac{D_{eff}}{D} = \frac{\varepsilon}{\tau}. \tag{16}$$

Hence, Bruggeman's model predicts a tortuosity factor of

$$\tau = \begin{cases} \varepsilon^{-1/2} & : n = 2 \quad \text{(spheres)} \\ \varepsilon^{-1} & : n = 1 \quad \text{(cylinders)} \end{cases} \tag{17}$$

for random porous media. Likewise, the same embedding procedure is applicable when considering electronic or ionic conductivity through the solid phase of a porous medium. Here, the ansatz is analogue to the case presented above, as the electron/ion transport through the porous phase is negligible. Hence, the final equation holds for transport phenomena through either phase, as long as the remaining phase is insulating and Bruggeman's assumptions are adhered to.

Discussion

One of the first applications of the Bruggeman correlation is found in the 1950s, where Hoogschagen (1955) measured gas diffusion through glass spheres and observed that values for the tortuosity factor lie between the Maxwell and Bruggeman correlation [18]. De La Rue and Tobias (1959) achieved similar results when measuring the effective conductivity values of an electrolyte solution impeded by the presence of non-conducting spheres [31].

The ease of application of this correlation means that it is still widely utilised to date, with particular recent emphasis in battery and fuel cell research. Its validity, however, remains the source of some dispute.

Ebner et al. have used tomography and simulation techniques to image a range of battery electrode materials [32]. For characteristically spherical cathode materials, it was shown that calculated tortuosity factor values of imaged battery electrode samples are close to, but usually lie slightly above, the standard formulation of the Bruggeman correlation cf. Eqn 17. For these materials, there was no significant directional dependence of tortuosity (i.e. the effective transport parameters in the x, y and z direction were approximately equivalent). By contrast, for more heterogeneous structures, such as graphite anode materials, the non-sphericity led to a requirement for re-formulation of the Bruggeman exponent (achieved using differential effective medium methods). A noticeable anisotropy in directional tortuosity factor was observed for these samples, mandating the use of different Bruggeman exponents dependent on the direction of the effective transport measurement.

Chung et al. simulated microstructure of different particle size distributions and discovered that perfectly ordered particle distributions result in tortuosity factors close to, or below, the Bruggeman relation [33•].

Thorat *et al.* have utilized experimental AC impedance techniques to evaluate the transport properties of battery separator and electrode materials. In this case, the Bruggeman correlation systematically under-estimates the tortuosity factor for both, electrodes and separators, and they proposed an adapted form of the correlation to compensate for their findings, namely, by using a pre-exponential scaling factor [10].

We have also conducted extensive investigations, in particular using X-ray imaging and image based modelling, to establish the transport parameters for SOFC [34•], Li-ion battery electrodes [28•] and porous support layers of oxygen transport membranes [35], in all three cases noting significant deviation between the measured tortuosity factor and that predicted by Bruggeman. For all cases, the Bruggeman correlation significantly under-estimates the tortuosity for these complex, often heterogeneous material microstructures.

It is notable that the Bruggeman correlation, along with many other theoretical and empirical correlations [see Figure 4 for several models taken from a review by Shen and Chen [14]], provides a narrow 'band-width' of predicted tortuosity factors for porosity values in the range of 30–70%. As this range is co-incident with typical pore fractions for many working electrode systems, it is easy to mistake a coincidental similarity between measured and predicted tortuosity for a true correlation.

This uncertainty leads to the question: when is the Bruggeman correlation valid? The paragraphs above, and indeed the original constraints imposed by Bruggeman, infer that the Bruggeman relation is valid only in situations where the insulating phase is present in a low volume fraction and represented by random, isotropic spheres. The Bruggeman correlation cannot account for directional differences which may arise from non-spherical particle packings. The application of this correlation to determine tortuosity for non-ideal structures, such as those typically encountered in battery separators, anodes, fuel cell gas diffusion layers and SOFC electrodes should be applied with extreme caution, as similarities between predicted and measured tortuosity factor may be merely a coincidence, arising from the limited band-width for acceptable tortuosity factors in a porous media. In cases where the known microstructure is heterogeneous, the Bruggeman model can be rendered invalid, and more complex approaches are required to adequately characterise the transport properties of the material and its resultant tortuosity factor. These include image based modelling approaches using 3D microstructure data from tomography experiments [34•], [28•]. Where nano-scopic pore geometries influence the diffusion behaviour, because of more extensive Knudsen interactions, suitable modifications to image based models must be made to account for these non-continuum events. Information about molecular transport in meso-porous structures, for instance, can be obtained from Quasi-Elastic Neutron Scattering (QENS) [36].

Conclusion

Despite the frequent and enduring application of Bruggeman's correlation, the original derivation of its most popular form (Eqn 17), which relates the tortuosity factor to porosity, does not appear in the original manuscript. Here we revisit the effective medium theory based derivation and restate some of its key limitations. It is imperative to keep three points in mind when quantifying the tortuosity factor via Eqn 17:

1. The Bruggeman model is based on simple diffusive transport and the resulting tortuosity factor value should be used with care in more complex transport regimes.
2. There is no unique mapping of the Bruggeman model onto a purely geometric definition of the tortuosity factor, which needs to be considered when analysing tomography data with a view to digitally extracting transport properties.
3. The Bruggeman model assumes that the obstructions to transport consist of either spheres or cylinders and it appears to perform better when applied to media that resemble one of these morphologies.

Figure 4
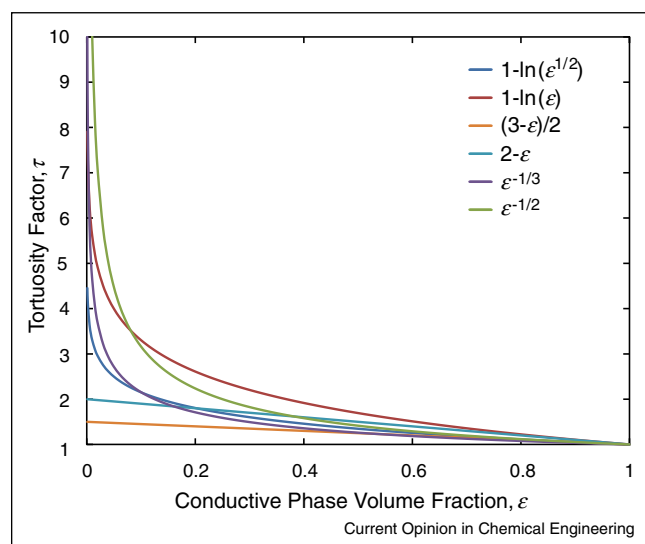
Comparison of several effective medium theory based porosity/tortuosity correlations taken from Shen and Chen [14].

References and recommended reading

Papers of particular interest, published within the period of review, have been highlighted as:

- • of special interest

1. Crank J: **The Mathematics of Diffusion**. Oxford: Clarendon Press; 1975.

2. Bruggeman VD: **Berechnung verschiedener physikalischer konstanten von heterogenen substanzen. i. dielektrizitätskonstanten und leitfähigkeiten der mischkörper aus isotropen substanzen**. *Ann Phys* 1935, **416**:636-664.

3. Lorentz H: **Ueber die beziehung zwischen der fortpflanzungsgeschwindigkeit des lichtes und der körperdichte**. *Ann Phys* 1880, **245**:641-665.

4. Lorenz L: **Ueber die refractionsconstante**. *Ann Phys* 1880, **247**:70-103.

5. Rayleigh L: **On the influence of obstacles arranged in rectangular order upon the properties of a medium**. *Philos Mag Ser 5* 1892, **34**:481-502 http://dx.doi.org/10.1080/14786449208620364.

6. Mackay TG, Lakhtakia A: **A limitation of the Bruggeman formalism for homogenization**. *Opt Commun* 2004, **234**:35-42 http://dx.doi.org/10.1016/j.optcom.2004.02.007 WOS:000220708100006.

7. Chalapat K, Timonen JV, Huuppola M, Koponen L, Johans C, Ras RH, Ikkala O, Oksanen MA, Seppala E, Paraoanu GS: **Ferromagnetic resonance in co-magnetic composites**. *Nanotechnology* 2014, **25**:485707 http://dx.doi.org/10.1088/0957-4484/25/48/485707 http://www.ncbi.nlm.nih.gov/pubmed/25397945.

8. Cernuschi F, Ahmaniemi S, Vuoristo P, Mantyla T: **Modelling of thermal conductivity of porous materials: application to thick thermal barrier coatings**. *J Eur Ceram Soc* 2004, **24**:2657-2667 http://dx.doi.org/10.1016/j.jeurceramsoc.2003.09.012 WOS:000222117300014.

9. Yang AK, Wang CA, Guo R, Huang Y: **Microstructure and electrical properties of porous PZT ceramics fabricated by different methods**. *J Am Ceram Soc* 2010, **93**:1984-1990 http://dx.doi.org/10.1111/j. 1551-2916.2010.03684.x WOS:000278914500031.

10. Thorat IV, Stephenson DE, Zacharias NA, Zaghib K, Harb JN, Wheeler DR: **Quantifying tortuosity in porous Li-ion battery materials**. *J Power Sources* 2009, **188**:592-600 http://dx.doi.org/10.1016/j.jpowsour.2008.12.032 WOS:000264646900039.

11. Kehrwald D, Shearing PR, Brandon NP, Sinha PK, Harris SJ: **Local tortuosity inhomogeneities in a lithium battery composite electrode**. *J Electrochem Soc* 2011, **158**:A1393-A1399 http://dx.doi.org/10.1149/2.079112jes WOS:000297979300022.

12. Ebner M, Wood V: **Tool for tortuosity estimation in lithium ion
  • battery porous electrodes**. *J Electrochem Soc* 2015, **162**:A3064-A3070 http://dx.doi.org/10.1149/2.0111502jes http://jes.ecsdl.org/content/162/2/A3064.full.pdf , WOS:000349014700005.
The authors present a tortuosity calculation software called 'BruggemanEstimator' which calculates the Bruggeman exponent and in turn, the tortuosity factor, based solely on 2D images. In comparison with numerical methods of extracting the tortuosity factor, high accuracy is achieved.

13. Ciuchi IV, Olariu CS, Mitoseriu L: **Determination of bone mineral volume fraction using impedance analysis and Bruggeman model**. *Mater Sci Eng B Adv Funct Solid-State Mater* 2013, **178**:1296-1302 http://dx.doi.org/10.1016/j.mseb.2013.04.001 WOS:000327285800006.

14. Shen L, Chen ZX: **Critical review of the impact of tortuosity on diffusion**. *Chem Eng Sci* 2007, **62**:3748-3755 http://dx.doi.org/10.1016/j.ces.2007.03.041 WOS:000248141200010.

15. Clennell MB: **Tortuosity: a guide through the maze**. *Dev Petrophys* 1997, **122**:299-344 http://dx.doi.org/10.1144/gsl.sp.1997.122.01.18 WOS:A1997BJ70H00018.

16. Ghanbarian B, Hunt AG, Ewing RP, Sahimi M: **Tortuosity in porous media: a critical review**. *Soil Sci Soc Am J* 2013,

77:1461-1477 http://dx.doi.org/10.2136/sssaj2012.0435 https://www.soils.org/publications/sssaj/abstracts/77/5/1461 , WOS:000324626600001.

17. Maxwell JC, Thompson JJ: **A Treatise On Electricity and Magnetism**. Clarendon; 1892.

18. Hoogschagen J: **Diffusion in porous catalysts and adsorbents**. *Ind Eng Chem* 1955, **47**:906-912.

19. Chueh CC, Bertei A, Pharoah JG, Nicolella C: **Effective conductivity in random porous media with convex and non-convex porosity**. *Int J Heat Mass Transfer* 2014, **71**:183-188 http://dx.doi.org/10.1016/j.ijheatmasstransfer.2013.12.041 WOS:000332438400020.

20. Mench MM: *Fuel Cell Engines*. John Wiley and Sons; 2008.

21. Jiang Y, Virkar AV: **Fuel composition and diluent effect on gas transport and performance of anode-supported SOFCS**. *J Electrochem Soc* 2003, **150**:A942-A951 http://dx.doi.org/10.1149/1.1579480 WOS:000183508100017.

22. Das PK, Li XG, Liu ZS: **Effective transport coefficients in PEM fuel cell catalyst and gas diffusion layers: beyond Bruggeman approximation**. *Appl Energy* 2010, **87**:2785-2796 http://dx.doi.org/10.1016/j.apenergy.2009.05.006 WOS:000279710500004.

23. Pharoah JG, Karan K, Sun W: **On effective transport coefficients in PEM fuel cell electrodes: anisotropy of the porous transport layers**. *J Power Sources* 2006, **161**:214-224 http://dx.doi.org/10.1016/j.jpowsour.2006.03.093.

24. Newman J, Tiedemann W: **Porous-electrode theory with battery applications**. *AIChE J* 1975, **21**:25-41.

25. Shearing PR, Eastwood DS, Bradley RS, Gelb J, Cooper SJ, Tariq F, Brett DJ, Brandon NP, Withers PJ, Lee PD: **Exploring electrochemical devices using X-ray microscopy: 3D microstructure of batteries and fuel cells**. *Microsc Anal* 2013, **27**.

26. Ebner M, Geldmacher F, Marone F, Stampanoni M, Wood V: **X-ray tomography of porous, transition metal oxide based lithium ion battery electrodes**. *Adv Energy Mater* 2013, **3**:845-850 http://dx.doi.org/10.1002/aenm.201200932 WOS:000327698200005.

27. Stephenson DE, Hartman EM, Harb JN, Wheeler DR: **Modeling of particle–particle interactions in porous cathodes for lithium-ion batteries**. *J Electrochem Soc* 2007, **154**:A1146-A1155 http://dx.doi.org/10.1149/1.2783772 WOS:000250504600012.

28. Cooper SJ, Eastwood DS, Gelb J, Damblanc G, Brett DJL,
  • Bradley RS, Withers PJ, Lee PD, Marquis AJ, Brandon NP, Shearing PR: **Image based modelling of microstructural heterogeneity in LiFePO$_4$ electrodes for Li-ion batteries**. *J Power Sources* 2014, **247**:1033-1039 http://dx.doi.org/10.1016/j.jpowsour.2013.04.156 WOS:000328177000136.
This is the first study applying X-ray tomography and simulation techniques to LFP batteries, which compares the tortuosity factors derived from a heat flux simulation with values extracted via the Bruggeman correlation. Even though the Bruggeman correlation is widely used in battery research, the presented data suggest that the Bruggeman correlation underestimates the tortuosity factor values in this case.

29. Epstein N: **On tortuosity and the tortuosity factor in flow and diffusion through porous-media**. *Chem Eng Sci* 1989, **44**:777-779 http://dx.doi.org/10.1016/0009-2509(89)85053-5 WOS:A1989T339200030.

30. Wiener OH: **Die theorie des mischkörpers für das feld der stationären strömung. 1. abhandlung: Die mittelwertsätze für kraft, polarisation und energie**. BG Teubner; 1912.

31. De La Rue RE, Tobias CW: **On the conductivity of dispersions**. *J Electrochem Soc* 1959, **106**:827-833.

32. Ebner M, Chung D-W, García RE, Wood V: **Tortuosity anisotropy in lithium ion battery electrodes studied by synchrotron X-ray tomography**. *J Electrochem Soc* 2013 http://dx.doi.org/10.1002/aenm.201301278.

33. Chung DW, Ebner M, Ely DR, Wood V, Garcia RE: **Validity of the
  • Bruggeman relation for porous electrodes**. *Modell Simul Mater Sci Eng* 2013, **21**:074009 http://dx.doi.org/10.1088/0965-0393/21/7/074009 WOS:000325585500010.

Using synchrotron X-ray tomography of differently manufactured porous battery electrodes in combination with computer generated porous structures, an extensive study on the validity of the Bruggeman correlation in porous membranes is carried out. The authors demonstrate that ordered computer generated samples show high correlation with the Bruggeman relation while spatial inhomogeneities in the manufactured samples feature higher tortuosity values than predicted by Bruggeman.

34. Cooper SJ, Kishimoto M, Tariq F, Bradley RS, Marquis AJ,
• Brandon NP, Kilner J, Shearing PR: **Microstructural analysis of an LSCF cathode using in-situ tomography and simulation**. *Solid Oxide Fuel Cells 13 (Sofc-Xiii)* 2013, **57**:2671-2678 http://dx.doi.org/10.1149/05701.2671ecst WOS:000338989005017.
In this article, the authors apply five different tortuosity factor calculation approaches from the literature to a porous SOFC cathode sample and compare the resulting values with the Bruggeman equation. Not only do the different tortuosity calculation methods slightly differ from each other, the Bruggeman relation appears to significantly underestimate the tortuosity factor for this sample.

35. Tjaden B, Lane J, Withers PJ, Bradley RS, Brett DJ, Shearing PR: **The application of 3d imaging techniques, simulation and diffusion experiments to explore transport properties in porous oxygen transport membrane support materials**. *Solid State Ionics* 2016 http://dx.doi.org/10.1016/j.ssi.2016.01.030.

36. Rives S, Jobic H, Beale A, Maurin G: **Diffusion of CH$_4$, CO$_2$, and their mixtures in ALPO4-5 investigated by QENS experiments and MD simulations**. *J Phys Chem C* 2013, **117**:13530-13539.